

Calcareous nannofossil biostratigraphy of the mudstone-limestone interbeds exposure in Northern Cement Corporation (NCC) Quarry, Sison, Pangasinan (Philippines)

Clarence Y. Magtoto* and Allan Gil S. Fernando

Nannoworks Laboratory, National Institute of Geological Sciences, University of the Philippines,
Diliman, Quezon City 1101 Philippines

(*Corresponding author: renz_y_magtoto@yahoo.com; agsfernando@yahoo.com)

Abstract This study aims to establish the calcareous nannofossil biostratigraphy of the mudstone-limestone interbeds inside the property of Northern Cement Corporation (NCC) in Sison, Pangasinan, northern Luzon of the Philippines. The interbeds are part of the Ilocos-Central Luzon Basin, which have been the subject of earlier nannofossil biostratigraphic studies. Analysis of 135 mudstone samples shows generally moderately- to well-preserved nannofossil assemblages. Based on the presence of the marker taxa *Discoaster berggrenii*, *Discoaster quinquenarius*, *Discoaster surculus*, *Amaurolithus primus*, *Reticulofenestra rotaria*, and *Discoaster loeblichii*, Nannofossil Zones NN11A to NN11B were recognized, suggesting an age of late Miocene (Tortonian to Messinian) for the mudstone-limestone interbeds. Lithologic and biostratigraphic comparisons with previously mapped lithologic units in the study area suggest that the interbeds belong to the Amlang Formation and its upper age limit may be extended to late late Miocene.

Key words: Calcareous nannofossil, biostratigraphy, Ilocos-Central Luzon Basin, Amlang Formation, Philippines

Introduction

The province of Pangasinan (Luzon Island, Philippines) is located within the Ilocos-Central Luzon Basin, a north-south oriented basin running from Ilocos Norte southwards to Metro Manila (Fig. 1). The basin is filled with up to 8,000m-thick sedimentary sequence composed of Oligocene to Pleistocene sediments derived from the Luzon Central Cordillera Range (to the east) and Zambales Mountain Range (to the west), and deposited in a wide range of marine environments (Saldivar-Sali (1978), Maletterre (1989) and Pinet and Stephan (1990) in Mines and Geosciences Bureau (MGB), 2010).

Previous studies recognize Zigzag Formation, Kennon Limestone, Klondyke Formation, Amlang Formation, Labayug Limestone, Mirador Limestone, Cataguintingan Formation, and Damortis Formation in the vicinity of Pangasinan

(Lorentz, 1984; Fernandez, 1996; Peña, 2008; MGB, 2010; Fig. 2). Detailed calcareous nannofossil biostratigraphic studies along Marcos Highway (Benguet Province) by De Leon and Militante-Matias (1992) and De Leon *et al.* (1998) assigned an age of late middle Miocene to early late Miocene (Nannofossil Zones NN5–NN10) for the Klondyke Formation. Likewise, Guballa and Fernando (2015) studied a section along Pugo River and assigned an age of middle late Miocene (Nannofossil Zone NN11A) for Amlang Formation. Fernandez (1996), on the other hand, used planktonic foraminifera biostratigraphy on samples from Labayug Limestone and assigned an age of late Miocene (Foraminiferal Zone N17).

Despite these studies, the sedimentary units in the Ilocos-Central Luzon Basin have not yet been subjected to detailed biostratigraphic studies. This is now being addressed by recent fieldworks

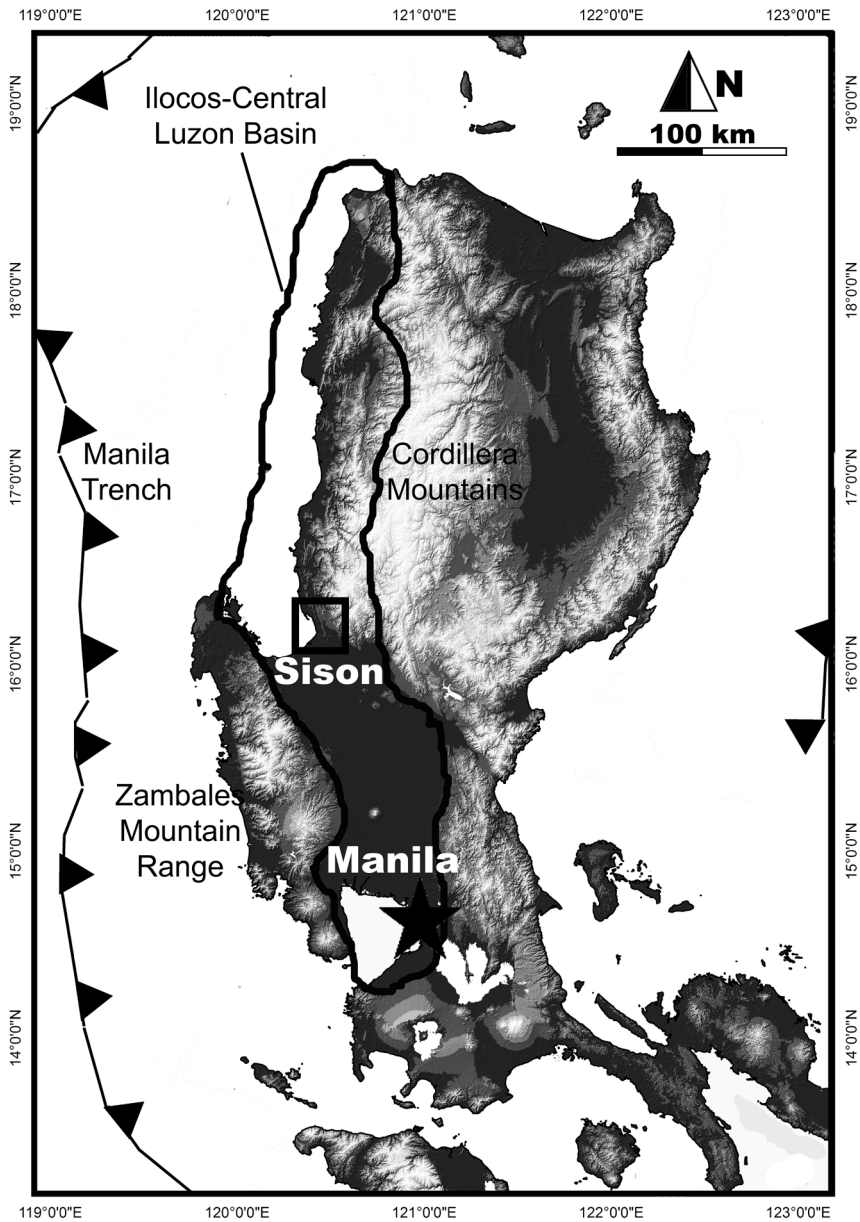


Fig. 1. Location map of the study area (Sison, Pangasinan). The black outline along the western coast of Luzon Island demarcates the Ilocos-Central Luzon Basin.

in the area by members of the Nannoworks Laboratory of the National Institute of Geological Sciences, University of the Philippines (UP NIGS). One of the areas currently being investigated is the mudstone-limestone interbeds (locally known as “shale quarry”) inside the Northern Cement Corporation (NCC) property in

Sison, Pangasinan. Fernandez (1996) previously mapped the mudstone-limestone interbeds as part of the late Miocene Amlang Formation due to its gradational contact with the underlying Labayug Limestone. This study reports the results of the calcareous nannofossil biostratigraphic analysis of samples taken from the mudstone-limestone

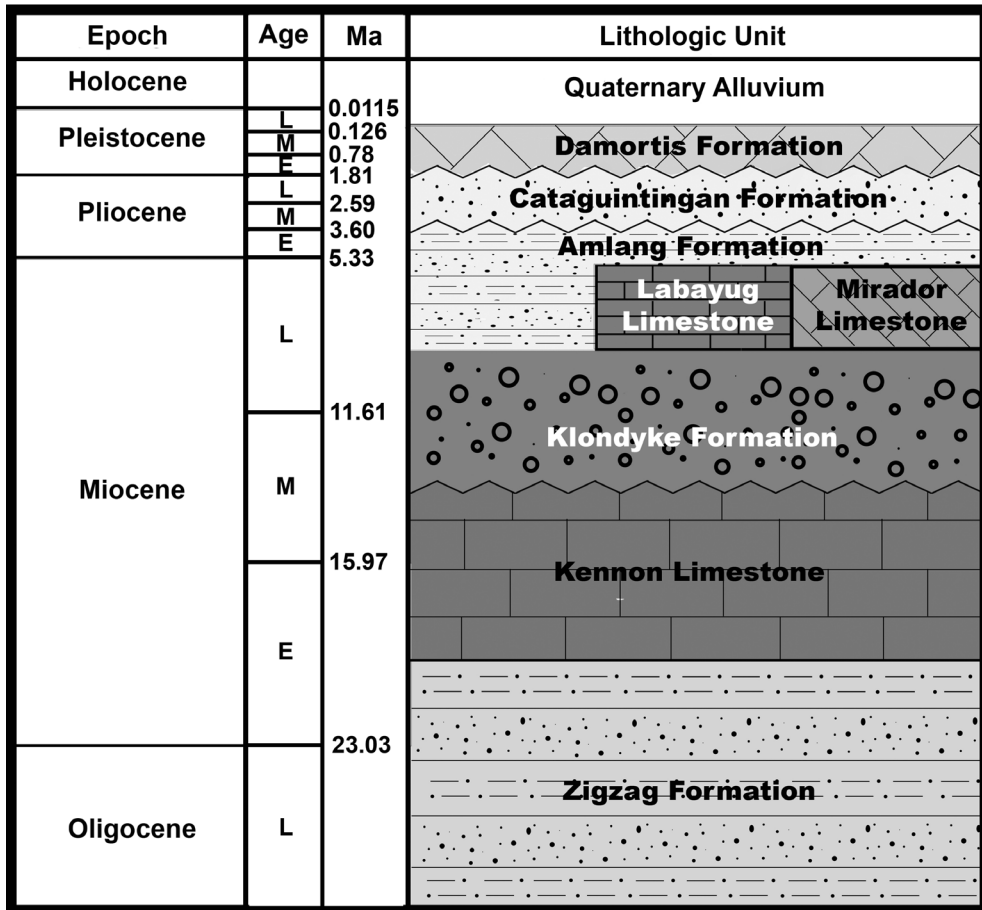


Fig. 2. Generalized stratigraphic column of the Ilocos-Central Luzon Basin at the vicinity of Sison, Pangasinan. The mudstone-limestone interbeds of NCC were previously assigned to the Amlang Formation based on lithological characteristics and depositional setting (Fernandez, 1996). Figure modified from Peña (2008).

interbeds of the NCC.

Study Area

The NCC Quarry area is located in the central part of the Ilocos-Central Luzon Basin (Fig. 1). The basin is tectonically controlled by the strike-slip Vigan-Aggao Fault (the northern segment of the Philippine Fault) in the east, and the Manila Trench in the west (Pinet and Stephan, 1990; MGB, 2010; Arfai *et al.*, 2011). The Ilocos-Central Luzon Basin is dominated by marine sedimentary sequences (MGB, 2010; Arfai *et al.*, 2011). Provenance studies suggest that the late Oligocene-middle Miocene sediments in the

northern part of the basin originated from the Central Cordillera Range (Lorentz, 1984; Pinet and Stephan, 1990; Faustino-Eslava *et al.*, 2013). These are overlain by late Miocene-Pliocene sedimentary sequences consisting mainly of sandstones, shales, carbonates and tuffaceous deposits. In the southern part of the basin, middle Miocene turbidites overlie sediments that originated from the Zambales Ophiolite Complex at the western side, while volcanic sediments and carbonates were deposited at the eastern side (MGB, 2010; Arfai *et al.*, 2011).

As mentioned previously, the NCC mudstone-limestone interbeds were previously mapped as part of the Amlang Formation, which consists of

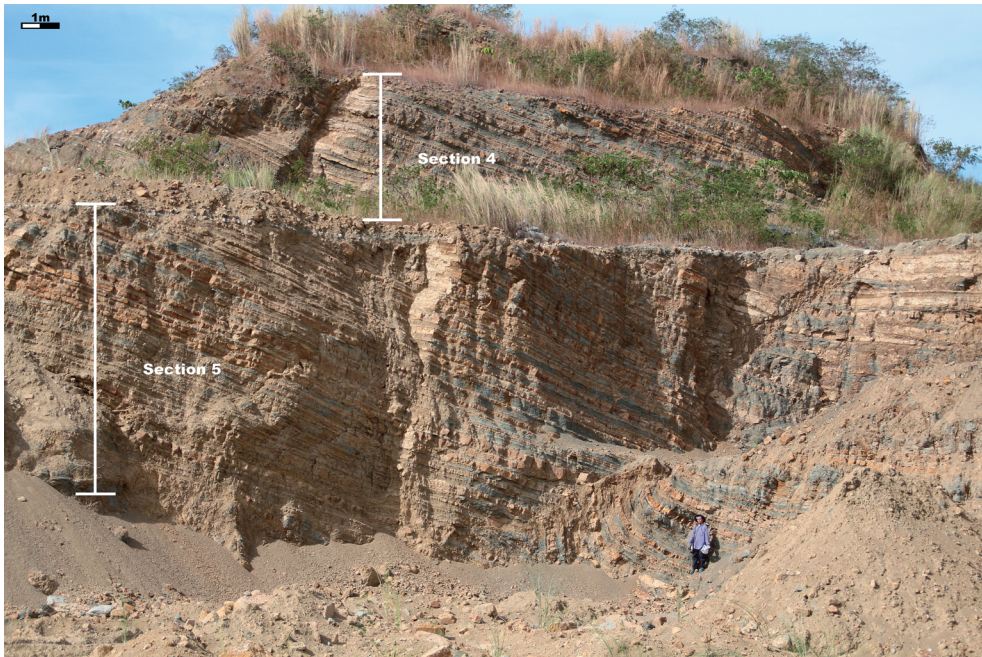


Fig. 3. Exposure of the mudstone-limestone interbeds of the Northern Cement Corporation Quarry in Sison, Pangasinan showing Sections 4 and 5.

thinly-bedded shales interbedded with medium- to fine-grained sandstones with some pebbly sandstones, pyroclastics, and conglomerates deposited in a deep marine setting. The upper member of the formation, on the other hand, exhibit higher proportions of siltstones, sandstones, and pebble conglomerates which may indicate a transition to shallow marine settings (Lorentz, 1984; De Leon *et al.*, 1998; Peña, 2008; MGB, 2010).

The mudstone-limestone interbeds consist of mudstones, calcarenites, calcirudites, and poly-mictic conglomerates. Conglomerates dominate the bottom half of the section, while calcarenites and mudstones dominate the upper half (Figs. 3, 4). The beds strike NW and dip 10–45° NE. Sedimentary structures observed include normal and reverse-graded bedding, load casts, planar and wavy laminations, and horizontal and vertical burrows. Gastropod, bivalve, coral and leaf fossils were also observed.

Materials and Methods

A total of 135 mudstone samples were collected from several sections to establish the calcareous nannofossil biostratigraphy of the mudstone-limestone interbeds (Fig. 4). The standard method outlined by Bown (1998) was used to prepare smear slides from the mudstone samples. The smear slides were observed under a polarizing microscope at 1000× magnification with at least 400 fields of view (FOV) observed per sample. Specimens were identified down to the species level as much as possible using images illustrated and described in Bolli and Saunders (1985), Bown (1998) and Young *et al.* (2017, Nannotax, <http://www.mikrotax.org/Nannotax3/>). The relative abundances of the species observed were recorded using the following categories: abundant (A), ≥ 25 specimen/FOV; very common (VC), 2-24 specimens/FOV; common (C), 1/1-5 FOVs; few (F), 1/6-10 FOVs; rare (R), 1/11-24 FOVs, and; very rare (VR), $1/\leq 25$ FOVs (see Appendix).

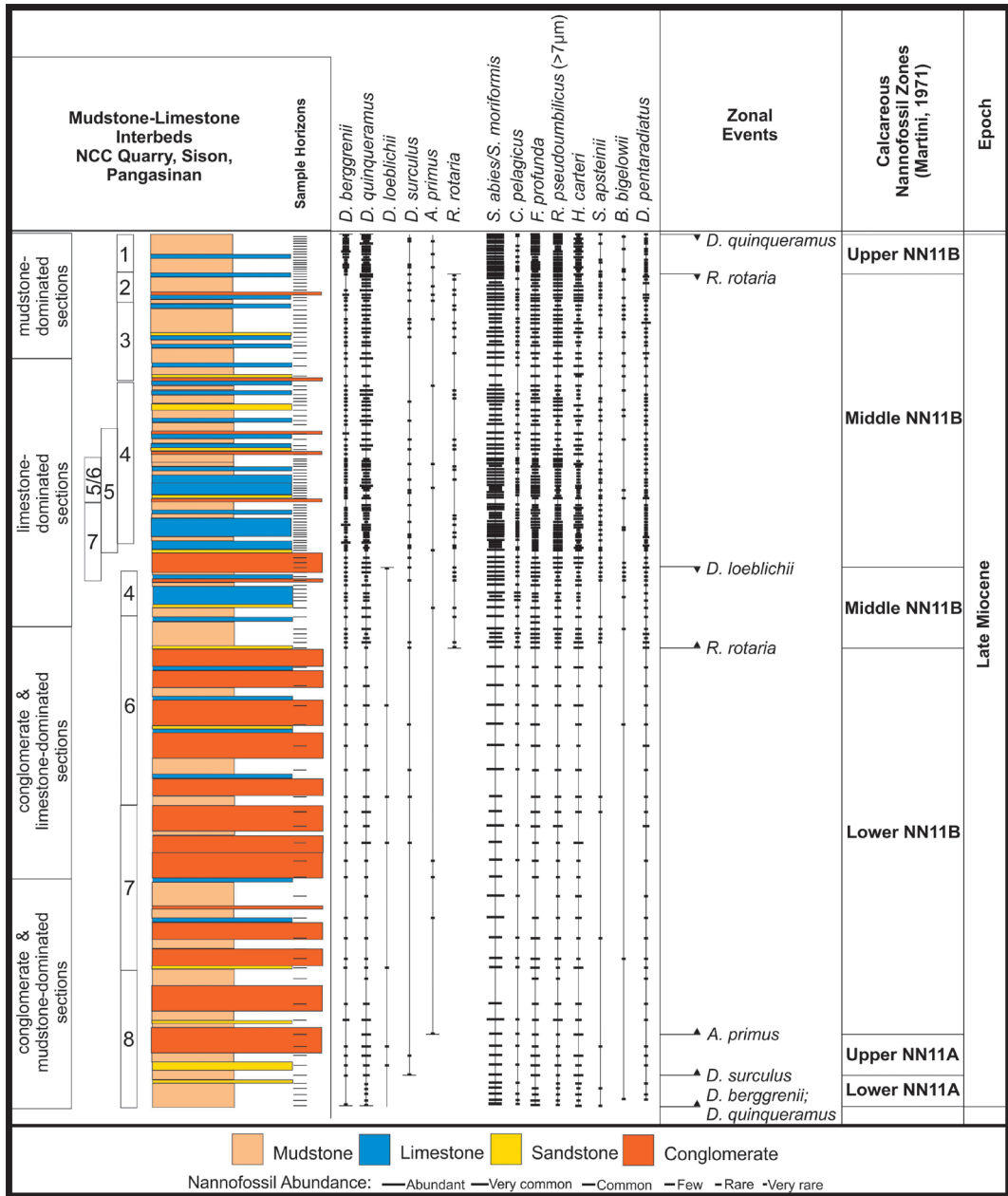


Fig. 4. Calcareous nannofossil biostratigraphic zonation and distribution of calcareous nannofossil zonal markers and other selected taxa in the mudstone-limestone interbeds of NCC Quarry area, Sison, Pangasinan. Thin horizontal bars at right side of the lithologic column indicate relative stratigraphic positions of the samples analyzed in this study (see also Appendix).

The nannofossil zones were established using the NN Zones of Martini (1971), supplemented by nannofossil events from Okada and Bukry (1980), and the recent studies of Backman *et al.*

(2012), Clemens *et al.* (2016), Raffi *et al.* (2016) and Rosenthal *et al.* (2017). Figure 5 shows comparison of the nannofossil zonation schemes by the aforementioned authors. Specimens of taxa

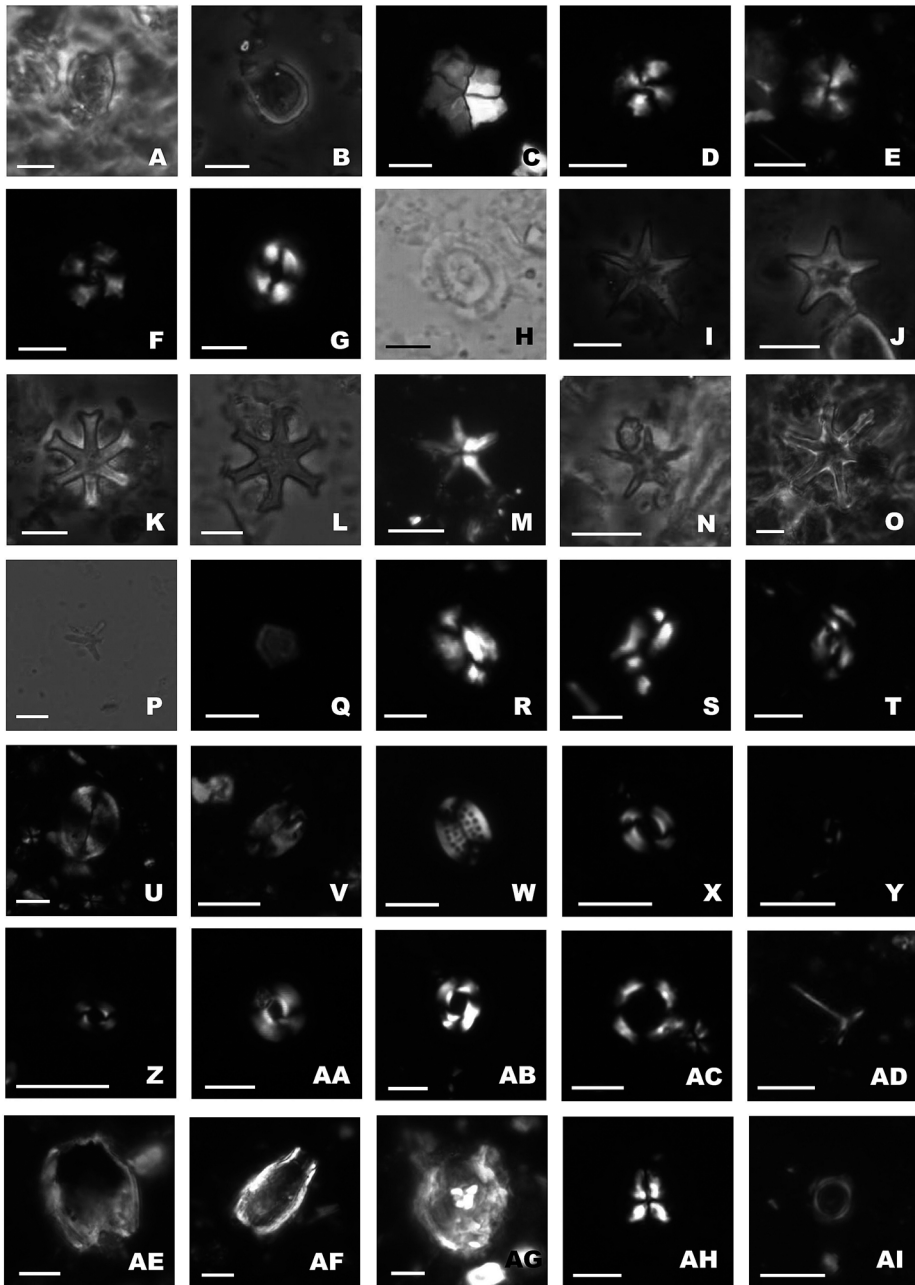


Fig. 5. Selected microphotographs of some taxa observed in the mudstone-limestone interbeds of Northern Cement Corporation (NCC) Quarry in Sison, Pangasinan, with XPL for cross-polarized images and PC for phase contrast images (scale bar = 5 μ m). **A**, *Amaurolithus delicatus*, PPL; **B**, *Amaurolithus primus*, PPL; **C**, *Braarudosphaera bigelowii*, XPL; **D**, *Calcidiscus leptoporus*, XPL; **E**, *Calcidiscus tropicus*, XPL; **F**, *Calcidiscus macintyreii*, XPL; **G–H**, *Coccolithus pelagicus*, XPL (G), PPL (H); **I**, *Discoaster bellus*, PPL; **J**, *Discoaster berggrenii*, PPL; **K**, *Discoaster challenger*, PPL; **L**, *Discoaster loeblichii*, PPL; **M**, *Discoaster pentaradiatus*, XPL; **N**, *Discoaster quinqueramus*, PPL; **O**, *Discoaster surculus*, PPL; **P**, *Discoaster triradiatus*, PPL; **Q**, *Florisphaera profunda*, XPL; **R–S**, *Helicosphaera carteri*, XPL; **T**, *Helicosphaera intermedia*, XPL; **U**, *Pontosphaera discopora*, XPL; **V**, *Pontosphaera japonica*, XPL; **W**, *Pontosphaera multipora*, XPL; **X**,

Age(Ma)	GPTS	Epoch	Stage	Calcareous Nannofossil Zones			Biohorizons	
				Okada & Bukry, 1980	Martini, 1971	Backman et al., 2012		
5.0	C3n	Late Miocene	Messinian	CN10b	NN12	CNP1	<i>C. acutus</i> TRZ	▲ <i>Ceratolithus acutus</i> (5.36)
	C3r			CN10a		CNM20	<i>T. rugosus</i> PRZ	▼ <i>Discoaster quinqueramus</i> (5.53)
6.0	C3An			CN9b	CNM19	<i>D. quinqueramus</i> TZ	▼ <i>Reticulofenestra rotaria</i>	
	C3Ar				CNM18	<i>N. amplificus</i> TRZ	▼ <i>Nicklithus amplificus</i> (5.98)	
7.0	C3Br				NN11	CNM17	<i>A. primus</i> BZ	▼ <i>Discoaster loeblichii</i>
	C4n		CNM16	<i>D. berggrenii</i> BZ		▲ <i>Nicklithus amplificus</i> (6.82)		
8.0	C4r		Tortonian	CN9a	NN10	CNM15	<i>D. bellus</i> BZ	▲ <i>Reticulofenestra rotaria</i>
	C4Ar					CNM14	<i>R. pseudoumbilicus</i> PRZ	▲ <i>Amaurolithus primus</i> (7.39)
9.0	C4n			CN8b	NN9	CNM13	<i>D. hamatus</i> TRZ	▼ <i>Discoaster surculus</i>
	C4r			CN8a		CNM13	<i>D. hamatus</i> TRZ	▲ <i>Discoaster berggrenii</i> (8.20)
10.0	C5n	CN7		CNM13	<i>D. hamatus</i> TRZ	▲ <i>Ba Reticulofenestra pseudoumbilicus</i> (8.80)		
					▼ <i>Discoaster hamatus</i> (9.65)			
					▲ <i>Discoaster hamatus</i> (10.49)			

Fig. 6. Comparison of the calcareous nannofossil zonation schemes by Martini (1971), Okada and Bukry (1980), and Backman *et al.* (2012). Figure modified from Raffi *et al.* (2016).

observed, particularly the marker taxa used for age determination, were photographed using the software Image-Pro Plus 7.0 attached to the Olympus BX51 polarizing microscope. Samples, smear slides and original nannofossil images are stored at the Nannoworks Laboratory of UP NIGS and the Macropaleontology Laboratory of the National Museum of Nature and Sciences, Tsukuba.

Results and Discussion

The calcareous nannofossil assemblages are generally moderately- to well-preserved. A total of 54 species divided into 14 genera were observed in the samples (Appendix). Most of the species observed belong to the following genera: *Calcidiscus*, *Coccolithus*, *Discoaster*, *Florisphaera*, *Helicosphaera*, *Reticulofenestra*, *Pontosphaera*, *Scyphosphaera*, *Sphenolithus* and *Umbilicosphaera*. Figure 4 shows the occurrence trends of marker taxa and some more commonly occurring taxa observed in the samples analyzed. Figure 5 shows the images of marker and com-

monly occurring taxa along with the images of rarer taxa observed in the samples used.

Based on the recognition of the first occurrence (FO) of *Amaurolithus primus*, Nannofossil Zones NN11A and NN11B were recognized. Secondary nannofossil markers, in addition, were used to establish informal subdivisions (i.e., lower, middle, upper) and will be discussed later. The zones identified are: (1) lower NN11A (*Discoaster berggrenii*/*Discoaster quinqueramus*-*Discoaster surculus* base zone); (2) Upper NN11A (*Discoaster surculus*-*Amaurolithus primus* base zone); (3) lower NN11B (*Amaurolithus primus*-*Reticulofenestra rotaria* base zone); (4) middle NN11B (*Reticulofenestra rotaria*-*Discoaster loeblichii* concurrent range zone, and (5) upper NN11B (*Reticulofenestra rotaria*-*Amaurolithus primus* top zone (Fig. 6). The zones are discussed in detail below.

Lower NN11A (middle late Miocene)

The interval is defined by the FOs of *Discoaster berggrenii*, *Discoaster quinqueramus* in the lower part of section 8 and the FO of *Dis-*

Reticulofenestra haqii, XPL; **Y**, *Reticulofenestra minuta*, XPL; **Z**, *Reticulofenestra minutula*, XPL. **AA**, *Reticulofenestra pseudoumbilicus* <7 µm, XPL; **AB**, *Reticulofenestra pseudoumbilicus* >7 µm, XPL; **AC**, *Reticulofenestra rotaria*, XPL; **AD**, *Rhabdosphaera clavigera*, XPL; **AE**, *Scyphosphaera apsteinii*, XPL; **AF**, *Scyphosphaera lagena*, XPL; **AG**, *Scyphosphaera* XPL.

coaster surculus in the middle part of section 8 (Fig. 4). The FO of *D. surculus* is a supplementary datum within the Nannofossil Zone NN11A (Young, 1998), and is also a secondary datum within CNM16 (Backman *et al.*, 2012). This zone partially corresponds to the lower CN9a of Okada and Bukry (1980) and lower CNM16 of Backman *et al.* (2012) (Fig. 6). In Aubry (2015), however, the FO of *D. surculus* is synchronous with the FOs of *D. quinqueramus* and *D. berggrenii*.

Upper NN11A (middle late Miocene)

The interval is defined by the FO of *Discoaster surculus* and the FO of *Amaurolithus primus* in the upper part of section 8 (Fig. 4). The FO of *A. primus* is a primary marker separating Nannofossil Zones NN11A and NN11B (Young, 1998; Aubry, 2015), as well as a primary marker for the top of CNM16/base of CNM17 (Backman *et al.*, 2012). This zone corresponds to the upper CN9a of Okada and Bukry (1980) and upper CNM16 of Backman *et al.* (2012) (Fig. 6).

Lower NN11B (late late Miocene)

The interval is bounded by the FO of *Amaurolithus primus* and the FO of *Reticulofenestra rotaria* in the upper portion of section 6 (Fig. 4). The FO of *R. rotaria* is a supplemental marker within Nannofossil Zone NN11B (Young, 1998), but is considered as a primary marker in Clemens *et al.* (2016). In Backman *et al.* (2012), the top of CNM17 is defined by the FO of *Nicklithus amplificus*, which was not observed in the samples. The FO of *R. rotaria* (6.91 Ma), however, is close to the FO of *Nicklithus amplificus* (6.82 Ma) and, therefore, can be used to approximate the top of CNM17 (Clemens *et al.*, 2016; Raffi *et al.*, 2016). This zone partially corresponds to the lower CN9b of Okada and Bukry (1980) and CNM17 of Backman *et al.* (2012) (Fig. 6).

Middle NN11B (late late Miocene)

This interval can be further subdivided into: (a) a lower part which is bounded by the FO of *R. rotaria* and LO of *Discoaster loeblichii* in the

upper portion of section 7; and (b) an upper part bounded by the LO of *D. loeblichii* and LO of *R. rotaria* in the upper portion of section 2 (Fig. 4). Similar to the FO, the LO of *R. rotaria* is a supplemental marker for the upper portion of Nannofossil Zone NN11B in Young (1998), but is used as a primary marker in Clemens *et al.* (2016) for the same interval.

The LO of *D. loeblichii* was shown to occur within Nannofossil Zone NN11B (Young, 1998). In Rosenthal *et al.* (2017), on the other hand, the LO of *D. loeblichii* occurs below the FO of *A. primus*, which is the marker for the boundary between Nannofossil Zones NN11A and NN11B, CNM16 and CNM17, and CN9a and CN9b. This discrepancy could be due to variations in taxonomic concept or reworking which prompted Young *et al.* (2017) to caution about using the LO of *D. loeblichii* as marker. In the present study, the moderately-preserved state of *D. loeblichii* (Fig. 5) suggests that reworking is unlikely. The LO of *R. rotaria* (5.94 Ma) is close to the LO of *N. amplificus* (5.98 Ma) and, therefore, can be used to approximate the base of CNM19 (Clemens *et al.*, 2016; Raffi *et al.*, 2016). It should be noted that the LOs of *R. rotaria* and *D. loeblichii* are not used either as primary or secondary markers in Backman *et al.* (2012), Aubry (2015), and Raffi *et al.* (2016). The middle NN11B zone, therefore, corresponds to the middle CN9b of Okada and Bukry (1980) and CNM18 Backman *et al.* (2012) (Fig. 6).

Upper NN11B (late late Miocene)

This interval is bounded by the LO of *R. rotaria* and the uppermost occurrence of *D. quinqueramus* at the top of the section 1 (Fig. 4). In Young (1998), Backman *et al.* (2012), Aubry (2015), Clemens *et al.* (2016), Raffi *et al.* (2016), and Rosenthal *et al.* (2017), the LO of *D. quinqueramus* is considered as a primary marker for the boundary of Nannofossil Zones NN11B and NN12, CNM19 and CNM20, and CN9b and CN10. *Amaurolithus primus* was also observed near the top of section 1, but because the LO of *A. primus* occurs at higher biostratigraphic zones

(NN14), it was not used in this study. This zone, therefore, corresponds to the upper CN9b of Okada and Bukry (1980) and CNM19 of Backman *et al.* (2012) (Fig. 6).

Comparison with Previous Studies

The age of the mudstone-limestone interbeds established in the present study correlates well with results of previous biostratigraphic studies near the study area. De Leon and Militante-Matias (1992) assigned the Klondyke Formation to the Nannofossil Zones NN5–NN10 (late middle Miocene to middle late Miocene), while De Leon *et al.* (1998) assigned an age of NN11 to exposures of the Amlang Formation in Benguet and La Union. Another section of the Amlang Formation along Pugo River in La Union was assigned by Guballa and Fernando (2015) to NN11A (middle late Miocene). These results supports the gradational contact between the Klondyke Formation and the Amlang Formation reported in previous studies (De Leon and Militante-Matias, 1992; Fernandez, 1996; De Leon *et al.*, 1998).

This study suggests that the basal portion of the mudstone–limestone interbeds of NCC could be partially contemporaneous with the Pugo River section studied by Guballa and Fernando (2015), implying continuous deposition during the late Miocene (NN11A to NN11B). The age is also consistent with the age of the Labayug Limestone, which is reported to be contemporaneous with the lower portion of the Amlang Formation (Fernandez, 1996; De Leon *et al.*, 1998). The Labayug Limestone was dated by Fernandez (1996) to planktonic foraminifera zone N17 (late Miocene).

The Labayug Limestone is considered reefal (Fernandez, 1996), while the limestones in the mudstone–limestone interbeds were interpreted as allodapic. The latter is supported by sedimentary structures supporting transport (i.e., soft sedimentary deformation structures and normal grading), as well as the fragmentary nature of reef-derived bioclasts mixed with lithic fragments and detrital minerals. Therefore, the mud-

stone-limestone interbeds in the NCC Quarry Area cannot be assigned to the Labayug Limestone. Rather, as recognized by Fernandez (1996) and De Leon *et al.* (1998), the mudstone-limestone interbeds can be assigned to the Amlang Formation (Fig. 2) based on similarities in general lithology (thinly-bedded shales interbedded with medium to fine-grained sandstones with some pebbly sandstones, pyroclastics, and conglomerates) and depositional setting (deep marine setting).

Fernandez (1996) hypothesized that the Labayug Limestone drowned during the late Miocene and contributed to the deposition of the mudstone-limestone interbeds. This supports the conclusions of earlier studies about the depositional setting of the Amlang Formation, which is in a bathyal environment (Lorentz, 1984; De Leon and Militante-Matias, 1992). The observed occurrence of fossilized leaves and carbonized stems in some mudstones and calcarenites suggests that there could be also be a significant terrestrial influence at the time of deposition.

Conclusions

1. The present study assigns the mudstone-limestone interbeds in the NCC Quarry (Sison, Pangasinan) to the Nannofossil Zones NN11A and NN11B (middle to late late Miocene). This is based on the presence of the marker taxa *Discoaster berggrenii*, *Discoaster quinqueramus*, *Discoaster surculus*, *Amaurolithus primus*, *Reticulofenestra rotaria*, and *Discoaster loeblichii*. Based on the lithological characteristics and the inferred deep marine depositional setting, the mudstone-limestone interbeds can be included as part of the Amlang Formation;

2. The established nannofossil zones for the mudstone-limestone interbeds is consistent with the earlier assigned nannofossil zones for the Amlang Formation (De Leon and Militante-Matias, 1992; De Leon *et al.*, 1998; Guballa and Fernando, 2015). The Nannofossil Zone NN11A (middle late Miocene) age assignment to the basal portion of the mudstone-limestone inter-

beds suggests that it is partially contemporaneous with the Pugo River section investigated by Guballa and Fernando (2015).

3. The allodapic characteristics of the limestones in the study area suggest that the carbonate source for the sediment was probably the adjacent Labayug Limestone. The presence of fossilized plant remains in the mudstone and limestone beds suggests significant terrestrial influence in the depositional area despite its deep marine setting.

Acknowledgements

We would like to thank the personnel of the Northern Cement Corporation (Engr. Alfred Ballasteros, Jr., Vice President Oliver Gorrospe, Ms. Myra Vanessa Frijellana) for permission, use of facilities, and assistance provided during the surveys of the study area. We would also like to thank the graduate students (Jaan Ruy Conrad Nogot, Gretchen Callejo, Yvonne Ivy Doyongan) and student assistants of the Nannoworks Laboratory (Miguel Javier, Ralf Grandon Dy, Jica Domingo, Dyan Plata, Paul Flores, Jeremy Jimenez, Nelissa Prado, Shyrill Mae Mariano, Abigael Villaruel) for assisting in the collection of samples. Dr. Tomoki Kase is also acknowledged for reviewing the manuscript.

References

- Arfai, J., Franke, D., Gaedicke, C., Lutz, R., Schnabel, M., Ladage, S., Berglar, K., Aurelio, M., Montano, J. and Pellejera, N. (2011) Geological evolution of the West Luzon Basin (South China Sea, Philippines). *Marine Geophysical Research*, **32**: 349–362.
- Aubry, M. -P. (2015) Cenozoic Coccolithophores, Discoasterales. 431 pp. Micropaleontology Press, New York.
- Backman, J., Raffi, I., Rio, D., Fornaciari, E. and Pälike, H. (2012) Biozonation and biochronology of Miocene through Pleistocene calcareous nannofossils from low and middle latitudes. *Newsletters on Stratigraphy*, **45**: 221–244.
- Bolli, H. M. and Saunders, J. B. (1985) Oligocene to Holocene low latitude planktic foraminifera. In: Bolli, H. M., Saunders, J. B. and Perch-Nielsen, K. (Eds.), *Plankton Stratigraphy*, Vol. 1. University Press, Great Britain, pp. 155–262.
- Bown, P. R. (Ed.) (1998) *Calcareous Nannofossil Stratigraphy*. 315 pp. Chapman and Hall; Kluwer Academic Publishers, London.
- Clemens, S. C., Kuhnt, W., LeVay, L. J., and the Expedition 353 Scientists (2016). *Site U1447*. In: Clemens, S. C., Kuhnt, W., LeVay, L. J., and the Expedition 353 Scientists (Eds.), *Indian Monsoon Rainfall, Proceedings of the International Ocean Discovery Program*, 353. College Station, TX, pp. 1–30.
- De Leon, M. M. and Militante-Matias, P. J. (1992) Calcareous nannofossil biostratigraphy of the western part of Tarlac Province, Central Luzon Basin. *Journal of the Geological Society of the Philippines*, **47** (1-2): 35–92.
- De Leon, M. M., Militante-Matias, P. J. and Tamesis, E. V. (1998) Calcareous nannofossil biostratigraphy of the submarine fan sequence of the Klondyke and Amlang Formations in Benguet and La Union Provinces, Philippines. *Journal of the Geological Society of the Philippines*, **53** (4-5): 89–141.
- Faustino-Eslava, D. V., Dimalanta, C. B., Yumul, G. P. Jr., Servando, N. T., and Cruz, N. A. (2013) Geohazards, tropical cyclones and disaster risk management in the Philippines: adaptation in a changing climate regime. *Journal of Environmental Science and Management*, **16** (1): 84–97.
- Fernandez, M. V. (1996) Sediment facies, age, and depositional environments of the Labayug Limestone, Sison, Pangasinan. Unpublished Master Thesis, National Institute of Geological Sciences, College of Science, University of the Philippines. Th/CS-GE-96-50.
- Guballa, J. D. S., and Fernando, A. G. S. (2015) Calcareous nannofossil biostratigraphic study of the Pugo River section of Amlang Formation in the Luzon Central Valley Basin, Philippines. *Bulletin of National Science Museum of Tokyo, Series C*, **41**: 1–7.
- Lorentz, R. A. (1984) Stratigraphy and sedimentation of late Neogene sediments on the southwest flank of Luzon Central Cordillera, Philippines. *Journal of Philippine Geology*, **38**: 1–24.
- Maleterre, P. (1989) Contribution a l'etude geologique de la plaque mer des Philippines. Histoire sedimentaire magmatique, et metallogenique d'un arc cenozoique deforeme en regime de transpression. Unpublished Ph.D. Dissertation, University of Western Brittany, France.
- Martini, E. (1971). Standard Tertiary and Quaternary calcareous nannoplankton zonation. In: Farinacci, A. (Ed.), *Proceedings of the Second International Conference on Planktonic Microfossils*, 2. pp. 739–785.
- Mines and Geosciences Bureau (MGB) (2010). *Geology of the Philippines*, 2nd Edition. 532 pp. Mines and Geosciences Bureau, Quezon City.
- Okada, H. and Bukry, D. (1980) Supplementary modifica-

- tion and introduction of code numbers to the low-latitude coccolith biostratigraphic zonation (Bukry 1973, 1975). *Marine Micropaleontology* **5**: 321–325.
- Peña, R. E. (2008) *Lexicon of Philippine Stratigraphy 2008*. 346 pp. The Geological Society of the Philippines, Inc., Mandaluyong City, Philippines.
- Pinet, N. and Stephan J. F. (1990) The Ilocos Foothills and Western Central Cordillera: A Key Region for the Understanding of the Geodynamic Evolution of the Eurasian Margin in Luzon Area (Philippines). *Tectonics and Circum-Pacific Continental Margins*, pp. 165–180.
- Raffi, I., Agnini, C., Backman, J., Catanzariti, R. and Palike, H. (2016) A Cenozoic calcareous nannofossil biozonation from low and middle latitudes: A synthesis. *Journal of Nannoplankton Research*, **36** (2): 121–132.
- Rosenthal, Y., Holbourn, A. E., Kulhanek, D. K., and the Expedition 363 Scientists (2017) Expedition 363 Preliminary Report: Western Pacific Warm Pool, International Ocean Discovery Program. 69 pp. Texas A&M University, Texas. doi.org/10.14379/iodp.pr.363.2017
- Saldivar-Sali, A. (1978) Reef exploration in the Philippines. In: *Second Circum-Pacific Energy and Mineral Reservoir Conference*. Honolulu, Hawaii, Bureau of Energy Devison, ministry of Energy, The Philippines, p. 54.
- Young, J. R. (1998) Neogene. In: Bown, P. R. (Ed.), *Calcareous Nannofossil Stratigraphy*. Chapman and Hall; Kluwer Academic Publishers, London, pp. 226–265.
- Young, J. R., Bown, P. R. and Lees, J. A. (Eds.) (2017) *Nannotax3*. Retrieved 14 September 2017, from: <http://www.mikrotax.org/Nannotax3/index.html>.

Appendix. Continued.

Sample	Preservation	<i>Amaurillithus delicatus</i>	<i>Amaurillithus primus</i>	<i>Brauridoophaera bigelowii</i>	<i>Calcidiscus leptopus</i>	<i>Calcidiscus tropicus</i>	<i>Calcidiscus macintyrei</i>	<i>Coccolithus pelagicus</i>	<i>Discoaster bellus</i>	<i>Discoaster berggrenii</i>	<i>Discoaster bolli</i>	<i>Discoaster braunlii</i>	<i>Discoaster quinqueramus</i>	<i>Discoaster calcaris</i>	<i>Discoaster challengeri</i>	<i>Discoaster exilis</i>	<i>Discoaster loeblichii</i>	<i>Discoaster pentaradiatus</i>	<i>Discoaster prepenaradiatus</i>	<i>Discoaster surculus</i>	<i>Discoaster triadatus</i>	<i>Discoaster variabilis</i>	5-Rayed <i>Discoaster</i> spp.	6-Rayed <i>Discoaster</i> spp.	<i>Floerissphaera profunda</i>	
4C-035 BOTTOM	M-G	—	—	—	VR	VR	VR	VR	—	VR	—	—	F	—	VR	—	—	VR	—	—	VR	VR	VR	F		
7D-021	G	—	—	—	VR	VR	VR	VR	—	R	—	—	F	—	—	—	—	VR	—	VR	—	—	VR	VR	VR	
4C-029	M	—	—	VR	VR	VR	VR	VR	—	VR	VR	—	R-F	—	VR	—	—	VR	—	—	—	VR	VR	R		
4C-023	M	—	—	VR	VR	VR	VR	VR	—	VR	—	—	R	—	—	—	—	VR	—	—	—	VR	VR	R-F		
4C-017	M-G	—	—	—	VR	VR	VR	VR	—	VR	VR	—	R	—	VR	—	—	VR	—	—	—	VR	VR	R-F		
4C-009	M	—	—	—	VR	VR	VR	VR	—	VR	VR	—	R	—	VR	VR	—	VR	—	—	—	VR	VR	R		
7D-013	M	—	—	—	VR	VR	VR	VR	—	VR	VR	VR	F	—	VR	—	—	VR	—	VR	—	—	VR	R	VR	
4C-003	G	—	—	—	VR	VR	VR	VR	—	VR	VR	—	VR	—	VR	—	—	VR	—	VR	—	—	VR	—	F	
5A-008	G	—	VR	—	VR	VR	VR	VR	—	VR	VR	—	R	—	VR	VR	—	R	—	—	—	—	VR	R-F		
7D-009	M-G	—	—	—	VR	VR	VR	VR	—	VR	—	—	F	—	—	—	—	VR	—	—	—	VR	VR	VR		
5A-004	M-G	—	—	—	VR	VR	VR	VR	—	—	—	—	VR	—	—	—	—	VR	—	—	—	—	R	VR	R	
5A-001	M	—	—	—	VR	VR	VR	—	—	VR	VR	VR	R	—	—	—	R	—	VR	VR	—	—	VR	VR	R-F	
7D-004	M-G	—	—	—	VR	VR	VR	F	—	VR-R	VR	VR	VR	—	VR	—	VR	VR	VR	VR	—	—	VR	VR	VR	
7D-001	G	—	—	VR	VR	VR	VR	VR	—	VR	—	—	F	—	—	—	VR	VR	—	—	—	VR	VR	VR	VR	
4B-009	M	—	—	VR	VR	VR	VR	VR	—	VR	VR	VR	VR	—	—	—	VR	—	VR	—	—	VR	VR	F		
4B-007	M-G	—	—	VR	VR	VR	VR	VR	—	VR	VR	VR	VR	—	VR	—	VR-R	VR	—	—	—	VR	VR	R-F		
4B-005	M	—	—	VR	VR	VR	VR	VR	—	VR	VR	—	R-F	—	VR	—	R	—	VR	—	—	VR	VR	F		
4B-001	M	—	—	VR	VR	—	—	VR	—	VR	—	—	VR	—	—	—	VR	VR	—	VR	—	—	VR	VR	R-F	
4A-010	M	—	—	—	VR	VR	VR	VR	—	VR	—	—	VR	—	—	—	—	VR	—	—	—	—	VR	VR	R-F	
4A-005	M	—	—	—	VR	VR	VR	VR	—	VR	VR	—	F	—	VR	—	—	VR	—	VR	—	—	VR	VR	F	
4A-003	M-G	—	VR	VR	VR	VR	VR	VR	—	VR	VR	—	VR	—	—	—	—	VR	—	—	—	—	VR	VR	F	
6A-001c	M	—	—	—	VR	VR	—	—	—	VR	—	—	VR	—	—	—	—	VR	—	—	—	—	VR	—	VR	
6A-008	M	—	—	—	VR	VR	VR	VR	—	VR	—	—	VR	—	VR	—	—	VR	—	—	—	—	VR	VR	VR	
6A-014	P-M	—	—	—	VR	VR	VR	VR	—	VR	—	—	VR	—	—	—	—	VR	—	—	—	—	VR	VR	R	
6A-016b	M	—	—	VR	VR	VR	VR	VR	—	VR	—	—	VR	—	—	—	—	VR	VR	—	—	—	VR	VR	VR-R	
6A-020	M	—	—	—	VR	VR	VR	VR	—	VR	VR	—	VR-R	—	—	—	—	VR	—	—	—	—	VR	VR	R	
6A-024	M	—	—	—	VR	VR	R	R	—	VR	—	VR	R-F	—	—	—	VR	R	—	—	—	—	VR	VR	R	
6A-030	P-M	—	—	—	VR	VR	VR	VR	—	VR	VR	—	R	—	—	—	—	VR	—	—	—	—	VR	VR	R	
6A-038	P-M	—	—	—	VR	VR	VR	VR	—	VR	VR	VR	R	—	—	—	—	R	—	—	—	—	VR	VR	R	
6B-005	M	—	—	—	VR	VR	R-F	R	—	VR	VR	VR	VR	—	—	—	—	R-F	VR	VR	VR	—	VR	VR	R	
6B-004	M	—	—	—	VR	VR	VR	VR	—	VR	VR	VR	VR	—	—	—	VR	VR	VR	VR	—	—	VR	VR	R	
6B-003	P-M	—	—	—	R	VR	R	VR	—	VR	—	—	VR	—	—	—	—	VR	VR	—	—	—	VR	VR	R	
6B-001	M	—	—	—	VR	—	VR	R	—	VR	—	—	VR	—	—	—	—	VR	—	—	—	—	VR	—	VR	
6C-003	P-M	—	—	VR	VR	VR	R	R	—	R	VR	VR	F	—	—	—	VR	VR	—	—	—	—	VR	VR	VR	
6C-002b	M	—	—	—	VR	VR	VR	VR	—	VR	VR	—	R	—	VR	—	—	R	—	VR	—	—	VR	VR	R	
6C-001	M	—	—	—	VR	VR	VR	VR	—	VR	VR	—	R	—	—	—	—	VR	—	—	—	—	VR	VR	VR	
7A-006	M	—	—	—	VR	VR	VR	VR	—	VR	VR	VR	VR	—	—	—	—	R	—	VR	—	—	VR	VR	VR	
7A-004	P-M	—	VR	—	VR	VR	VR	VR	—	VR	—	—	R	—	—	—	—	VR	—	VR	—	—	—	VR	—	
7A-003	M	—	VR	—	VR	—	VR	VR	—	VR	—	VR	VR	—	—	—	—	VR	VR	—	—	—	VR	—	VR	
7A-002	P-M	—	—	—	R	VR	R	VR	—	VR	—	—	VR	—	VR	—	—	VR	—	—	—	—	—	VR	VR	
7A-001	P-M	—	—	—	VR	VR	VR	—	—	VR	VR	VR	VR	—	—	—	VR	R	VR	VR	VR	—	—	R	VR	
7B-003	P-M	—	—	—	—	—	—	—	—	—	—	—	VR	—	—	—	—	—	—	—	—	—	—	VR	—	
7B-002	M	—	VR	VR	VR	VR	VR	VR	—	VR	—	—	R-F	—	—	—	—	VR	—	—	—	—	—	VR	VR	VR
7B-001	M	—	—	—	VR	—	—	—	—	VR	—	—	VR	—	—	—	—	—	—	—	—	—	—	VR	—	
7C-003	P-M	—	—	—	—	VR	VR	VR	—	VR	—	—	VR	—	—	—	—	VR	—	—	—	—	—	VR	VR	VR
7C-002	M	—	—	VR	VR	VR	VR	—	—	VR	—	—	VR	—	—	—	VR	VR	—	—	—	—	VR	VR	VR	
7C-001	P-M	—	—	—	VR	VR	R	VR	—	VR	VR	—	VR	—	—	—	VR	VR	—	—	—	—	—	VR	VR	VR
8A-005	P	—	—	—	VR	VR	—	—	—	—	—	VR	VR	—	—	—	—	VR	—	—	—	—	—	VR	—	VR
8A-004	P	—	—	—	VR	VR	VR	VR	—	VR	—	VR	R-F	—	—	—	—	VR	—	—	—	—	—	VR	VR	VR
8A-003	P	—	—	—	—	—	—	VR	—	R	—	—	R-F	—	—	—	—	VR	—	—	—	—	—	VR	VR	VR
8A-002	P-M	—	VR	—	R	VR	VR	VR	—	—	VR	—	R	—	VR	—	—	VR	—	—	VR	—	—	R	VR	VR
8A-001	P	—	—	—	—	VR	VR	—	—	VR	—	—	R	—	—	—	—	VR	—	—	—	—	—	VR	VR	VR
8B-003	P-M	—	—	—	R-F	R-F	R-F	R-F	—	VR	VR	VR	F	—	VR	VR	VR	VR	—	VR	—	—	VR	R	R	R
8B-002	P	—	—	—	VR	VR	VR	VR	—	VR	VR	—	R	—	VR	—	—	VR	—	—	—	—	—	VR	VR	VR
8B-001	P	—	—	—	R	VR	VR	VR	—	VR	VR	—	R	—	—	—	—	VR	—	VR	—	—	—	VR	VR	VR
8C-010	M	—	—	—	VR	—	—	VR	—	—	—	—	VR	—	—	—	VR	VR	—	—	—	—	—	VR	VR	F
8C-007	M	—	—	—	VR	—	—	—	—	—	—	—	VR	—	—	—	—	—	—	—	—	—	—	VR	VR	R-F
8C-005	P-M	—	—	—	—	VR	—	VR	—	—	—	—	VR	—	—	—	—	VR	—	—	—	—	—	VR	VR	VR-R
8C-003	P-M	—	—	VR	VR	VR	VR	VR	—	—	—	—	VR	—	VR	—	—	—	—	—	—	—	—	VR	VR	F
8C-001	P-M	—	—	—	VR	—	VR	VR	—	VR	—	—	VR	—	—	—	—	—	—	—	—	—	—	VR	VR	F-C

